Astronomy
&
Astrophysics

Grain growth and dust settling in a brown dwarf disk

Gemini/T-ReCS[⋆] observations of CFHT-BD-Tau 4

D. Apai[1], I. Pascucci[1], M. F. Sterzik[2], N. van der Bliek[3], J. Bouwman[1], C. P. Dullemond[4], and Th. Henning[1]

[1] Max Planck Institute for Astronomy, Königstuhl 17, 69117 Heidelberg, Germany
e-mail: apai@as.arizona.edu
[2] European Southern Observatory, Casilla 19001, Santiago 19, Chile
[3] Cerro Tololo Inter-American Observatory, Casilla 603, La Serena, Chile
[4] Max Planck Institute for Astrophysics, PO Box 1317, 85741 Garching, Germany

Abstract. We present accurate mid-infrared observations of the disk around the young, bona fide brown dwarf CFHT-BD-Tau 4. We report GEMINI/T-ReCS measurements in the 7.9, 10.4 and 12.3 μm filters, from which we infer the presence of a prominent, broad silicate emission feature. The shape of the silicate feature is dominated by emission from 2 μm amorphous olivine grains. Such grains, being an order of magnitude larger than those in the interstellar medium, are a first proof of dust processing and grain growth in disks around brown dwarfs. The object's spectral energy distribution is below the prediction of the classical flared disk model but higher than that of the two-layer flat disk. A good match can be achieved by using an intermediate disk model with strongly reduced but non-zero flaring. Grain growth and dust settling processes provide a natural explanation for this disk geometry and we argue that such intermediate flaring might explain the observations of several other brown dwarf disks as well.

Key words. accretion, accretion disks – circumstellar matter – planetary systems: protoplanetary disks
– stars: individual: CFHT-BD-Tau 4 – stars: low-mass, brown dwarfs – stars: pre-main sequence

1. Introduction

Circumstellar disks play an important role in the formation and early evolution of stars (see, e.g. Shu et al. 1987), as well as in the subsequent formation of planetary systems (see, e.g. Lissauer 1993). Similarly to young stars, infrared excess emission was recently identified from brown dwarfs (Comerón et al. 2000; Muench et al. 2001; Liu et al. 2003; Jayawardhana et al. 2003a). The interpretation of this excess emission as a proof of substantial amount of dust confined into a disk, was strongly supported by millimetre-wavelength observations estimating the total mass of two brown dwarf disks being 0.4−6 $M_{\rm Jup}$ (Klein et al. 2003).

The detection of brown dwarf disks sets at least two very important questions: *how does the disk structure compare to that of the T Tauri disks? Can brown dwarf disks potentially form planetary systems?*

Recent studies investigated the mid-infrared photometry from about 15 brown dwarf disks aiming to determine the disk structure (see, e.g. Natta & Testi 2001; Apai et al. 2002; Pascucci et al. 2003; Mohanty et al. 2004; Walker et al. 2004). The two basic models used are the flat (Adams et al. 1988) and flared (opening angle increasing with the radius, Chiang & Goldreich 1997) disks. Due to their geometry the flared disks absorb a larger fraction of the stellar light. This additional energy is re-emitted at mid- and far-infrared wavelengths leading to a far-infrared bump often observed in the spectral energy distribution of T Tauri and Herbig Ae disks.

The flat and flared disk model predictions deviate strongly longwards of 15 μm. In spite of the lack of observations in this regime, there is mounting evidence that both disk structures can be found in brown dwarf disks.

The similarity of disk structures and stellar mass/disk mass ratios between young stars and brown dwarfs emphasizes the exciting question whether planet formation can take place in brown dwarf disks. The major steps leading to planet formation start by grain growth and dust settling. While the early phases of such grain coagulation has been recently observed in the disk atmosphere (e.g., Przygodda et al. 2003;

Letter to the Editor

van Boekel et al. 2003; Meeus et al. 2003) and in the disk mid-plane (e.g., Calvet et al. 2002; Testi et al. 2003; Natta et al. 2004) of young low- and intermediate-mass stars, no such observation could be performed for the much fainter brown dwarf disks.

In this letter we focus on the disk around the spectroscopically confirmed, non-accreting brown dwarf CFHT-BD-Tau 4 (Martín et al. 2001; Jayawardhana et al. 2003b, RA $04^h39^m47.3^s$ Dec $+26^h01'39''$ J2000) being the best-understood such object with measurements in the near-infrared (Liu et al. 2003; Martín et al. 2001), mid-infrared ISOCAM (Pascucci et al. 2003) and sub-millimetre regimes (Klein et al. 2003). Based on these photometry Pascucci et al. (2003) carried out the most detailed and systematic analysis of disk models. They excluded all but three models as possibilities: the single- or double-layered flat disk or the flared disk with inner rim. These two models differ in the far-infrared and in the presence of the 9.7 μm silicate feature. As a continuation of this effort we present new, accurate mid-infrared photometry for CFHT-BD-Tau 4 obtained by the recently installed T-ReCS camera. The filter bandpasses probe the region of the 9.7 μm silicate emission feature. Modeling the shape of this feature allows us to determine the disk structure and test the dust grain properties.

2. Observations, data reduction and results

The observations have been carried out on Jan. 2, 2004 using the T-ReCS mid-infrared detector mounted on the Gemini South 8 m-telescope in service mode. The plate scale was 0.09″/pixel with a field of view of about 29″ × 22″. Three filters were used with central wavelengths (50% transmission wavelengths) of 7.9 μm (7.39−8.08 μm), 10.38 μm (9.87−10.89 μm) and 12.33 μm (11.74−12.92 μm).

In order to eliminate the high thermal background the usual chopping/nodding technique was used with throws of 10″. The total on-source integration times were 12, 7 and 10 min for the filters 7.9, 10.4 and 12.3 μm. The data reduction has been carried out by using self-developed IDL routines. Each chopping pair has been inspected manually to ensure the exclusion of the frames suffering from strong detector signatures, such as sinusoidally modulated background noise. During this procedure we rejected about 10% of the chopping pairs. Because the object is undetected in the individual chopping pairs, our manual selection does not bias towards stronger or fainter source flux. After the manual inspection the high-quality frames have been averaged.

The CFHT-BD-Tau 4 observations suffered from imperfect tracking, which resulted in somewhat blurred images. The relatively bright source, however, could be identified also on subgroups of the images, allowing us to track and correct its position during the exposure. This correction proved that CFHT-BD-Tau 4 is neither extended nor elongated on the T-ReCS images and allowed more accurate photometry.

The flux calibration is based on the calibrator HD 92305 (γ Cha), which was observed several times during the night. In order to derive accurate flux densities for the calibrator we integrated its spectra as given by Cohen et al. (1999) within the 50% transmission levels of the T-ReCS filter set. The flux

measurements have been carried out by using aperture photometry with the IDL-adaptation of the DAOPHOT routine (Stetson 1987). To increase the accuracy of our photometry, we tested different aperture annuli. We found that the fluxes in the final two negative and one positive beams of the given source show consistent, slowly changing values for aperture radii between 0.9″−1.35″. The fluxes obtained in this aperture range with 1-pixel steps have been used to determine the count rates from the source. These count rates have been converted to absolute flux densities by comparing them to the mean of three count rate measurements of the standard star obtained by the corresponding aperture sizes.

The mid-infrared emission of this brown dwarf disk is unresolved at a spatial resolution of 0.3″. Our images prove that no adjacent mid-infrared object could have influenced the previous coarse-resolution ISOCAM photometry.

We find the following flux densities for CFHT-BD-Tau 4: $F_{7.9}$ = 42 ± 10 mJy, $F_{10.4}$ = 51.4 ± 2.6 mJy and $F_{12.3}$ = 47.1 ± 2.4 mJy. The final fluxes are the mean values over the aperture range, while the photometric error bars given are the maximum deviations from the mean value inside the aperture range combined with the calibration uncertainties. The large error bar on the $F_{7.9}$ measurement reflects the low atmospheric transparency and the short integration times. The excess emission at 10.4 μm filter is undoubtly marking a prominent 9.7 μm silicate feature.

3. Models and interpretation

In this section we compare the new T-ReCS observations to model predictions aiming to explore the dust properties and disk geometry. First, we will use the mid-infrared data to constrain the most dominant dust species. Then, we will apply this information to a set of self-consistent disk models with different geometries.

3.1. Dominant dust species

We model the dust composition by simply decomposing the observed mid-infrared (T-ReCS and ISOCAM) flux densities into the sum of a black body and a modified black body, representing the continuum emission and the optically thin component responsible for the emission feature. A similar approach has been used in Bouwman et al. (2001) and Meeus et al. (2003), and for the details of the fitting procedure we refer to those articles. The weighting factors of the two components and the common temperature have been fitted by using the Levenberg-Marquardt minimization. By introducing different optical constants to the optically thin component we tested dust grains of diverse types and sizes as possible dominant species. We note, that the pure black body component can also represent dust grains without spectral features in the mid-infrared regimes, such as carbonaceous materials. The weighting factor of the modified black body is proportional to the mass in the optically thin regime.

In our model we used silicates with olivine composition (FeMgSiO$_4$, Dorschner et al. 1995), the most abundant interstellar silicate species, as well as amorphous silica

(Spitzer & Kleinman 1960). For both species we fitted the observation using spherical grains with radii between 0.1 and 100 μm. Based on the χ^2 comparison we found, that the 2.0 μm-sized olivine grains provide the best fit to the observations. The best-fit temperature was 490 K and the total dust mass in the optically thin regime equaled to 0.1 lunar mass.

In order to put a qualitative constraint on the mass ratio of the large/small grains, we included a second optically thin component. We find, that the lower limit for the mass ratio of the 2.0 μm grains to the 0.1 μm ones in the optically thin disk regime is $m_{2.0}/m_{0.1} > 6$.

3.2. Self-consistent disk models

The fitting procedure described above has no self-consistent physical basis, but it provides a good indication for the dominant dust species. We confirm this information by using self-consistent disk models described in Dullemond et al. (2001), which are improved versions of models by Chiang & Goldreich (1997). In these models the radiation field of the central object together with the dust properties determine the disk flaring angle.

In Pascucci et al. (2003) we already applied these models for CFHT-BD-Tau 4 and compared several disk geometries. We excluded all but three models: single-layer flat disk, two-layer flat disk and flared disk with inner rim (*m4*, *m5* and *m9* in Pascucci et al. 2003). The main parameters of those and the following models are: brown dwarf luminosity $L_{BD} = 0.1 L_{\odot}$, mass $M_{BD} = 0.075 M_{\odot}$, temperature $T_{eff} = 2800$ K; the dust opacities are those of 0.1 μm astronomical silicates (Draine & Lee 1984). The outer radius was set to 50 AU, but our observations do not constrain this parameter. The presence of the 9.7 μm silicate feature arises from an optically thin disk layer (e.g., disk atmosphere). As the single-layer flat disk model lacks any optically thin component, this model can be immediately excluded. When comparing the *m9* flared and *m5* flat disk models, we find that none of them matches well the new observations as long as the 0.1 μm astronomical silicates are used as dust species. Thus, successfully fitting the detailed mid-infrared data requires the identification of the dust species and its typical grain size in addition to the disk structure.

Here we use the results of Sect. 3.1, namely, our guess of 2.0 μm olivine grains as the dominant dust species. When we apply 2.0 μm-sized amorphous olivine grains in the disk models, we find that the two-layer flat disk model (*m5*) reproduces the observations better than the flared disk model. The best fit, however, is reached by applying a disk model intermediate between the flat and flared disk models: as discussed in the Sect. 4 we artificially reduced the disk height by a factor of 4 to account for dust settling effects.

As an illustration of the influence of the main parameters and the stability of our results in Fig. 1 we show the best-fit models with flat and flared geometries in combination with interstellar-like 0.1 μm astronomical silicate grains, as well as the intermediately flaring disk model and 2 μm grains.

Throughout the modeling procedure we also varied the inclination i, the inner disk radius R_{in}, the exponent α of the
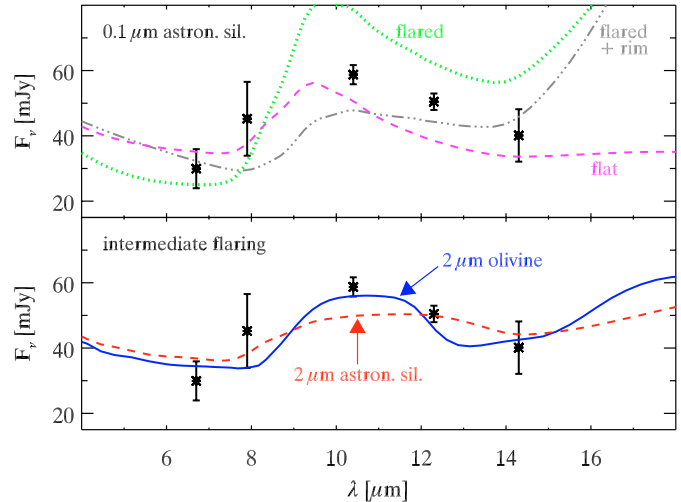

Fig. 1. Flat, flared and intermediate disk models compared to the observed spectral energy distribution of CFHT-BD-Tau 4. The upper panel has been calculated by using 0.1 astronomical silicate grains, while the lower panel applies 2.0 μm olivine and astronomical silicate grains. All model parameters are identical to those in Pascucci et al. (2003), except for the reduced flaring parameter of the intermediate model. The 850 μm and 1.3 mm observations are not shown here but fitted well, similarly to Pascucci et al. (2003). The best fit is achieved by the intermediately flaring model in combination with 2 μm amorphous olivine grains.

surface density power-law r^{α}, the presence of an inner rim and self-shadowing effects, the latter two being self-consistently calculated. The best solutions are found around the values of $i \simeq 0°$, $\alpha = -1.9$, $R_{in} = 3.5 R_{BD}$, and no inner rim.

Independently of the grain size estimate obtained by decomposing the emission feature, we also tried to fit the observations by using different dust species and geometries. However, no other configuration than a disk with reduced flaring and moderate-sized (2 μm) olivine grains could reproduce the measurements.

4. Discussion

4.1. Disk structure and dust settling

The sparsely sampled spectral energy distributions of the brown dwarf disks observed until now have been generally modeled by either flat or flared disk geometries. The flared disk models are based on the assumption of efficient mixing of gas and dust everywhere in the disk (Chiang & Goldreich 1997). In this picture the dust particles are kept above the disk midplane by the turbulent gas, which in turn is thermally coupled to the dust grains absorbing the incident stellar radiation. Grain growth, however, reduces the dust-gas coupling (Dubrulle et al. 1995; Dullemond & Dominik 2004) and accelerates the sinking of dust particles toward the disk midplane. Thus, the *dust* disk converges towards the flat disk geometry. Reduced disk scale heights have been argued for in the case of several disks around low- and intermediate-mass stars (see, e.g. Chiang et al. 2001).

Our modeling yields two major results: 1, the optically thin disk regime is dominated by at least intermediate-sized (~2 μm) dust grains; 2, the dust disk's scale height is strongly reduced.

These results are fully consistent with the evolution of disks through grain growth and subsequent settling, as outlined above. Up to now, this process has been only rarely observed in circumstellar disks and never in a disk of a brown dwarf. The multi-wavelength observations of the relatively bright disk of CFHT-BD-Tau 4 provide the first evidence that the similarity between young stars and brown dwarfs extends to circumstellar dust processing and the subsequent evolution of the disks.

We note here, that the picture of grain growth *and* dust settling might provide a natural explanation not only for CFHT-BD-Tau 4 but for several other brown dwarf disks with flat disks, such as Cha Hα2 (Apai et al. 2002), GY5 (Mohanty et al. 2004) and further 9 objects from (Natta & Testi 2001; Natta et al. 2002).

In Sect. 3.1 we estimated the mass in the optically thin regime to be ~0.1 lunar mass. The same method when applied to the sample of Herbig Ae stars presented in Bouwman et al. (2001) results in masses of ~100 lunar masses, about a thousand times larger than that of CFHT-BD-Tau 4. If these disks would be optically thin, their mid-infrared emission ratio would be similar to their mass ratio, i.e. ~50. The larger difference, however, is naturally explained if the emission originates from the atmosphere of an optically thick disk. In this case, the total emission scales with the surface area contributing to the 9.7 μm silicate feature: the radial dust temperature distribution in the disk atmosphere approximately scales as $T(r) \propto T_* \times (r)^{-\frac{2}{5}}$, where r is the radius, T_* is the stellar temperature, assuming the absorption coefficient κ to be $\propto \nu$. Given the typical Herbig Ae stellar temperatures being ~4 times larger than the corresponding brown dwarf temperatures, any given temperature around a brown dwarf is reached at ~30 times smaller radii compared to the Herbig Ae stars. This translates to a surface ratio of ~10^3, the same order of magnitude as the fitted mass ratios.

Our best-fit model – similarly to those of Natta & Testi (2001), Mohanty et al. (2004), Walker et al. (2004) and others – require an inner disk radius of $R_{\rm in} \simeq 3.2\, R_{\rm BD}$. This value is similar to the typical inner disk truncation radii deduced for T Tauri stars (Shu et al. 1994) and might be defined through dust sublimation at temperatures o ~1500 K.

4.2. Grain growth in a substellar disk

Our observations demonstrate that the disk atmosphere of CFHT-BD-Tau 4 is dominated by 2.0 μm grains, an order of magnitude larger than the average grains commonly found in the interstellar matter. Further modeling indicates that the grain growth is accompanied by dust settling. These two processes are the initial, essential steps of planet formation (Lissauer 1993).

Studies of coeval T Tauri disk systems showed that the dust evolutionary stage is only a weak function of time (see, e.g. Przygodda et al. 2003; Meeus et al. 2003). On the other hand, the rate of dust processing is likely to provide a useful way to parameterize the evolution of an accretion disk through protoplanetary disk into a debris disk. Comparing the derived $m_{2.0}/m_{0.1}$ ratio to those estimated for disks of Herbig Ae stars (Bouwman et al. 2001) provides some insight into the stage of the dust evolution in CFHT-BD-Tau 4. The values range from $m_{2.0}/m_{0.1} < 0.04$ for the unprocessed dust in the Galactic Centre up to >57 for the evolved disk of HD 100546. The $m_{2.0}/m_{0.1} > 6$ ratio of CFHT-BD-Tau 4 indicates that this brown dwarf disk is close in dust evolution phase to the 5 Myr-old HD 104237 (Grady et al. 2004). The fact, that comets Halley and Hale-Bopp show the presence of smaller grains ($m_{2.0}/m_{0.1} < 3$), might suggest that they formed in a dust evolutionary phase – but not necessarily in time – *prior* to that of CFHT-BD-Tau 4.

We directly derive the feature strength from the observations following Przygodda et al. (2003) and compare its ~1.6 value with the T Tauri star samples of Meeus et al. (2003) and Przygodda et al. (2003). This model-independent comparison again shows CFHT-BD-Tau 4 among the disks with the most processed dust.

The young age of CFHT-BD-Tau 4 (~1 Myr, Martín et al. 2001) stands intuitively in contrast to the evolved stage of its dust disk. There are three factors which may resolve this apparent contradiction: first, large differences in dust processing timescales have been spotted among T Tauri and Herbig Ae stars, indicating that dust processing can proceed at very different rates. Second, the over-luminosity of CFHT-BD-Tau 4 may be explained by an unresolved binary brown dwarf. Dynamical perturbations could then influence the dust coagulation and settling timescales. Hints for this behavior have been found in T Tauri disks (Meeus et al. 2003) and other brown dwarf disks (Sterzik et al. 2004). Third, if it is a binary system, then the age of CFHT-BD-Tau 4 is likely to be underestimated.

The only previous detection of silicate emission from a brown dwarf disk was found for the ρ Ophiucus object GY310 (Mohanty et al. 2004). In that case the shape of the feature hints on small dust grains, but the data quality do not allow any firm conclusion. Spectroscopic surveys with the new Spitzer Space Telescope will be able to derive the accurate dust composition for a large number of brown dwarf disks revealing how frequent grain growth processes are. However, to follow the grain growth to scales larger than a few micron, high-resolution (sub)millimetre observations are necessary, possibly by using interferometric facilities such as the Sub-millimeter Array or ALMA.

5. Summary

The main conclusions of this work are the following:

1. Using the T-ReCS/Gemini instrument we detected thermal infrared emission at 7.9 μm, 10.4 μm and 12.3 μm from the disk of CFHT-BD-Tau 4.
2. The disk displays a prominent silicate emission peak which proves the existence of an optically thin disk layer.
3. We compare the shape of the silicate emission feature to laboratory spectra emerging from different dust species and

grain sizes. Using two independent methods we find that the emission feature is dominated by 2 μm amorphous silicate (olivine) grains.

4. Simple semi-analytical models explain the observations by a two-layered flared disk with a reduced scale height. This transitionary disk model between flat and flared geometries is consistent with dust settling models.

5. The dominance of 2 μm grains and the reduced disk flaring prove that grain growth and settling occurred in the disk of the ~1 Myr-old CFHT-BD-Tau 4. Based on the derived mass ratio for the 2 μm to 0.1 μm grains the stage of dust processing in this brown dwarf disk is similar to that of the well-known Herbig Ae star HD 104237.

In view of these results we conclude, that the dust grain coagulation and dust settling, the initial steps of planet formation, take place in the disk of the brown dwarf CFHT-BD-Tau 4.

References

Adams, F. C., Shu, F. H., & Lada, C. J. 1988, ApJ, 326, 865
Apai, D., Pascucci, I., Henning, T., et al. 2002, ApJ, 573, L115
Bouwman, J., Meeus, G., de Koter, A., et al. 2001, A&A, 375, 950
Calvet, N., D'Alessio, P., Hartmann, L., et al. 2002, ApJ, 568, 1008
Chiang, E. I., & Goldreich, P. 1997, ApJ, 490, 368
Chiang, E. I., Joung, M. K., Creech-Eakman, M. J., et al. 2001, ApJ, 547, 1077
Cohen, M., Walker, R. G., Carter, B., et al. 1999, AJ, 117, 1864
Comerón, F., Neuhäuser, R., & Kaas, A. A. 2000, A&A, 359, 269
Dorschner, J., Begemann, B., Henning, T., Jaeger, C., & Mutschke, H. 1995, A&A, 300, 503
Draine, B. T., & Lee, H. M. 1984, ApJ, 285, 89
Dubrulle, B., Morfill, G., & Sterzik, M. 1995, Icarus, 114, 237
Dullemond, C. P., & Dominik, C. 2004, ArXiv Astrophysics e-prints
Dullemond, C. P., Dominik, C., & Natta, A. 2001, ApJ, 560, 957
Grady, C. A., Woodgate, B., Torres, C. A. O., et al. 2004, ApJ, 608, 809
Jayawardhana, R., Ardila, D. R., Stelzer, B., & Haisch, K. E. 2003a, AJ, 126, 1515
Jayawardhana, R., Mohanty, S., & Basri, G. 2003b, ApJ, 592, 282
Klein, R., Apai, D., Pascucci, I., Henning, T., & Waters, L. B. F. M. 2003, ApJ, 593, L57
Lissauer, J. J. 1993, ARA&A, 31, 129
Liu, M. C., Najita, J., & Tokunaga, A. T. 2003, ApJ, 585, 372
Martín, E. L., Dougados, C., Magnier, E., et al. 2001, ApJ, 561, L195
Meeus, G., Sterzik, M., Bouwman, J., & Natta, A. 2003, A&A, 409, L25
Mohanty, S., Jayawardhana, R., Natta, A., et al. 2004, ApJ, 609, L33
Muench, A. A., Alves, J., Lada, C. J., & Lada, E. A. 2001, ApJ, 558, L51
Natta, A., & Testi, L. 2001, A&A, 376, L22
Natta, A., Testi, L., Comerón, F., et al. 2002, A&A, 393, 597
Natta, A., Testi, L., Neri, R., Shepherd, D. S., & Wilner, D. J. 2004, A&A, 416, 179
Pascucci, I., Apai, D., Henning, T., & Dullemond, C. P. 2003, ApJ, 590, L111
Przygodda, F., van Boekel, R., Ábrahám, P., Melnikov, S. Y., Waters, L. B. F. M., & Leinert, C. 2003, A&A, 412, L43
Shu, F., Najita, J., Ostriker, E., et al. 1994, ApJ, 429, 781
Shu, F. H., Adams, F. C., & Lizano, S. 1987, ARA&A, 25, 23
Spitzer, W. G., & Kleinman, D. A. 1960, Phys. Rev., 121, 1324
Sterzik, M., Pascucci, I., Apai, D., van der Bliek, N., & Dullemond, C. P. 2004, A&A, in press
Stetson, P. B. 1987, PASP, 99, 191
Testi, L., Natta, A., Shepherd, D. S., & Wilner, D. J. 2003, A&A, 403, 323
van Boekel, R., Waters, L. B. F. M., Dominik, C., et al. 2003, A&A, 400, L21
Walker, C., Wood, K., Lada, C. J., et al. 2004, MNRAS, 351, 607

Letter to the Editor